Science and Technology Infusion Climate Bulletin
NOAA's National Weather Service
36th NOAA Annual Climate Diagnostics and Prediction Workshop
Fort Worth, TX, 3-6 October 2011

Dynamic Linkage between the Sahel Greening and Intense Atlantic Hurricanes

Shih-Yu Wang[1, 2] and Robert R. Gillies[1, 2]

[1]*Utah Climate Center, Utah State University, Logan, UT*

[2]*Department of Plants, Soils, and Climate, Utah State University, Logan, UT*

1. Introduction

Beginning around the early 1980s, the Sahel belt of Africa has undergone a continual increase in both precipitation and vegetation greening (Herrmann *et al.* 2005; Olsson *et al.* 2005). This so-called Sahel greening has been a signal of a gradual recovery from very dry conditions in the 1980s, and from the days of prolonged droughts and famines during the late 1960s–mid-1990s (Nicholson and Yin 2001; Dai *et al.* 2004). The increase in Sahel rainfall has been attributed to a combination of factors such as global warming (Lu and Delworth 2005; Hagos and Cook 2008), decadal-scale variability in the global sea surface temperature (SST) (Giannini *et al.* 2003; Hoerling *et al.* 2006; Cook 2008; Latif *et al.* 2010) and associated changes in the carbon cycle (Schimel *et al.* 2001). Previous studies have also pointed to a robust connection between the low-frequency rainfall variability in the Sahel and the Atlantic Multi-decadal Oscillation (AMO) – a basin-scale pattern of SST variability driven by Atlantic meridional overturning (Knight *et al.* 2005).

As shown in Fig. 1, the summer precipitation differences between 1995-2009 and 1979-1994 illustrates the northward displacement of the oceanic rainband that is connected to the wetness domain along the Sahel. Precipitation in the Sahel is produced through a set of complex interactions between different circulation systems – in particular, the Tropical Easterly Jet (TEJ) in the upper troposphere that extends from South Asia, the African Easterly Jet (AEJ) in the middle troposphere, and the tropical monsoon westerly in the lower troposphere that lies beneath the TEJ; these circulation features are depicted in Fig. 1. African Easterly Waves (AEWs) contribute to about 50% of the June-September rainfall in West Africa (Chen and Wang 2007). Moreover, AEWs are important precursors to intense hurricanes of Category 3 or above (Landsea and Gray 1992; Landsea 1993; Chen *et al.* 2008) and recent studies (Hopsch *et al.* 2007; Fink et al. 2010) have found a positively correlated, yet fluctuating relationship between the tropical cyclone activity, the West African monsoon, and AEWs.

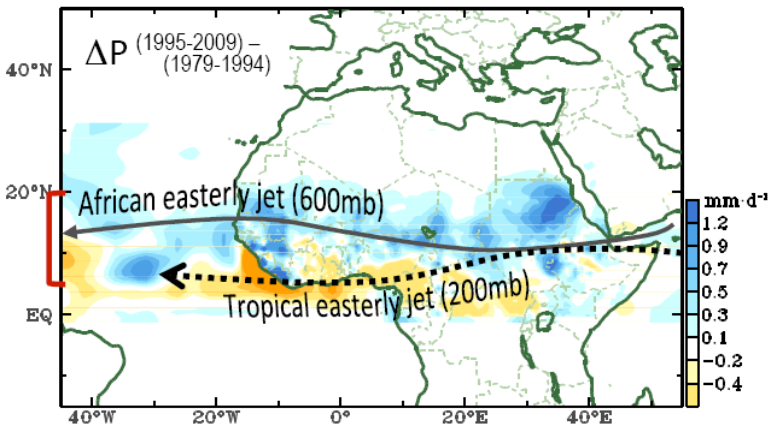

Fig. 1 July-August precipitation differences between the periods 1995-2009 and 1979-1994, from the University of Delaware data over land and the GPCP data over ocean. Jet cores along the African Easterly Jet and the Tropical Easterly Jet are indicated. The tropical monsoon westerly lies underneath the TEJ. The left boundary in red outlines the latitude zone used in Figs. 2-4.

Here we report a recent study by Wang and Gillies (2011) that examined the synoptic environment associated with the increasing precipitation in the Sahel. We also investigated the extent of any downstream effects the Sahel climate change has had on the increase in tropical cyclone threat (Emanuel 2005, 2007). Precursors to the analysis were first the adoption of several precipitation datasets and different generation global reanalyses as described in Section 2. The analysis in Section 3 is followed by a discussion of the

Correspondence to: Shih-Yu (Simon) Wang, Utah Climate Center & Department of Plants, Soils, and Climate, Utah State University, Logan, UT; E-mail: simon.wang@usu.edu.

temporal-spatial evolutions of prescribed meteorological variables and their links to Atlantic tropical cyclones. Concluding remarks are presented in Section 4.

2. Data sources

Our study utilized three sets of precipitation data: the Climate Prediction Center (CPC) Merged Analysis of Precipitation (CMAP; Xie and Arkin 1997), the Global Precipitation Climatology Project (GPCP) version 2 (Adler *et al.* 2003), and gauge-based precipitation compiled by the University of Delaware (UDel) (Legates and Willmott 1990). For verification purposes, we adopted the un-interpolated version of outgoing longwave radiation (OLR) measured from NOAA's polar orbiting satellites. For sea surface temperatures we utilized the NOAA Extended Reconstructed SST V3b (Smith and Reynolds 2003); for surface temperatures over land we used the CRU Air Temperature Anomalies Version 3 (*Brohan et al.* 2006) with the time period up to present. In the later part of the study we examined the occurrences of Atlantic tropical cyclones. Information of tropical cyclones was obtained from two sources: 1) the Atlantic Hurricane Dataset Re-analysis Project (Landsea *et al.* 2004) for the period 1979-2009, and 2) the National Hurricane Center's Tropical Prediction Center for 2010.

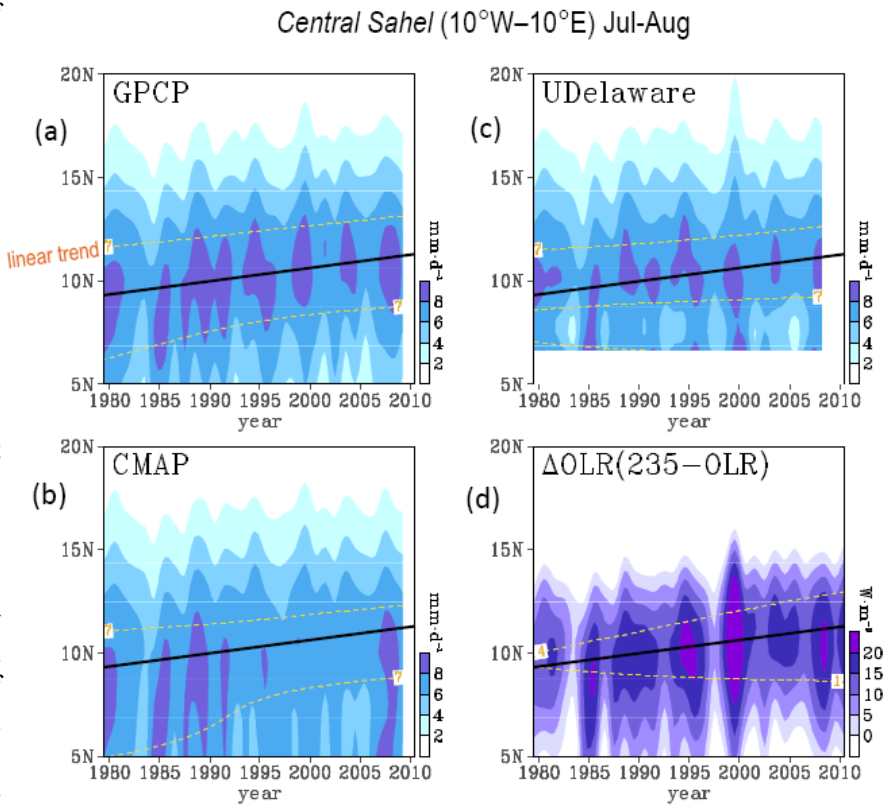

Fig. 2 Latitude-time profiles of precipitation averaged between 10°W and 10°E for the July-August season, derived from (a) GPCP, (b) CMAP, (c) University of Delaware, and (d) ΔOLR (= 235 Wm^{-2} – OLR). Yellow dashed lines are linear trends of the designated value. The solid black lines indicate the average latitudinal position of maximum precipitation for the depiction of the Sahel rainband.

Five global reanalysis datasets (hereafter referred to as reanalyses) were utilized: (1) the National Centers for Environmental Prediction/National Center for Atmospheric Research Global Reanalysis (NCEP1; Kalnay *et al.* 1996), (2) the NCEP/Department of Energy Global Reanalysis II (NCEP2) – the improved version of NCEP1 that included additional satellite-derived atmospheric information and newer physics schemes (Kanamitsu *et al.* 2002), (3) the European Centre for Medium-Range Weather Forecasts (ECMWF) 40-yr Reanalysis (ERA-40; Uppala *et al.* 2005), (4) the ERA-Interim reanalysis (Simmons *et al.* 2007), and (5) the Modern Era Retrospective-analysis for Research and Applications (MERRA) developed by NASA (Rienecker *et al.* 2011). All of the reanalyses are daily means. Because ERA-40 is only available up to 2002, the period 1989-2010 was merged with ERA-Interim by interpolating ERA-Interim's higher resolution onto ERA-40's 2.5° resolution through a bilinear approach. This merged reanalysis is referred to as ERA40/I.

3. Results

a. Changes in the Sahel climate

The change of precipitation during July-August (*i.e.* Sahel's rainy season) of 1979-2010 is illustrated in Fig. 2 as latitude-time diagrams of GPCP, CMAP, UDel and ΔOLR (=235 Wm^{-2} – OLR), averaged between 10°W and 10°E representing the central Sahel. A clear northward shift is revealed in these precipitation data

and proxy, without a discernable change in the amount (as inferred from the parallel trends). This feature is indicative of the fact that the increasing Sahel rainfall is not an expansion of the seasonal rainband but rather is a result of a positional shift. On the other hand, ΔOLR reveals a noticeable increase in magnitude in the precipitation condition (as noted from the diverging trends), suggestive of an intensification in the convective activity within the migrating rainbands. The latitudinal shift of the rainfall maximum – averaged from all four datasets – amounts to about +1.1° over the 32 year period and is indicated by the solid black line in Fig. 2. However, an examination of the model-generated precipitation from the four reanalyses (not shown) revealed a systematic bias that consisted of a southward displacement of the mean rainband (*i.e.* positioned at 7.5°N instead of 11°N as is the case in Fig. 2), without a discernable positional shift. Such reanalyses biases highlight a primary challenge of global climate models when it comes to producing reliable climate simulations and projections. For this reason we decided to use only the kinetic fields of the reanalyses.

Figure 3 shows changes in the TEJ, AEJ, and the tropical monsoon westerly in terms of zonal winds at (a) 200mb, (b) 600mb, and (c) 850mb, respectively, from the four reanalyses over the central Sahel. The point to note here is that there is a substantial increase in the TEJ and a slight southward shift of the jet core, although MERRA depicts less of a positional shift but does show a much stronger jet speed compared to the other reanalyses. NCEP2 and ERA40/I depict a similar structure of the TEJ but are somewhat different from the other reanalyses. Even though the TEJ has intensified, its southward expansion does not seem to correspond to the decreased tropical rainfall (south of 10°N; Fig. 2). For the AEJ (Fig. 3b), all the reanalyses, with the exception of MERRA, depict a northward shift of the jet consistent with the migrating rainband. Both NCEP2 and ERA40/I depict a clear intensification of the AEJ, whereas the intensification is weaker in NCEP1 and MERRA. For the tropical monsoon westerly, the reanalyses are somewhat divergent – while NCEP1 points to an increase in the westerly wind speed, ERA40/I indicates a sharp decrease. Nevertheless, all reanalyses agree upon a quasi-stationary behavior of the monsoon westerly. It appears that the four reanalyses exhibit somewhat different characteristics of the African

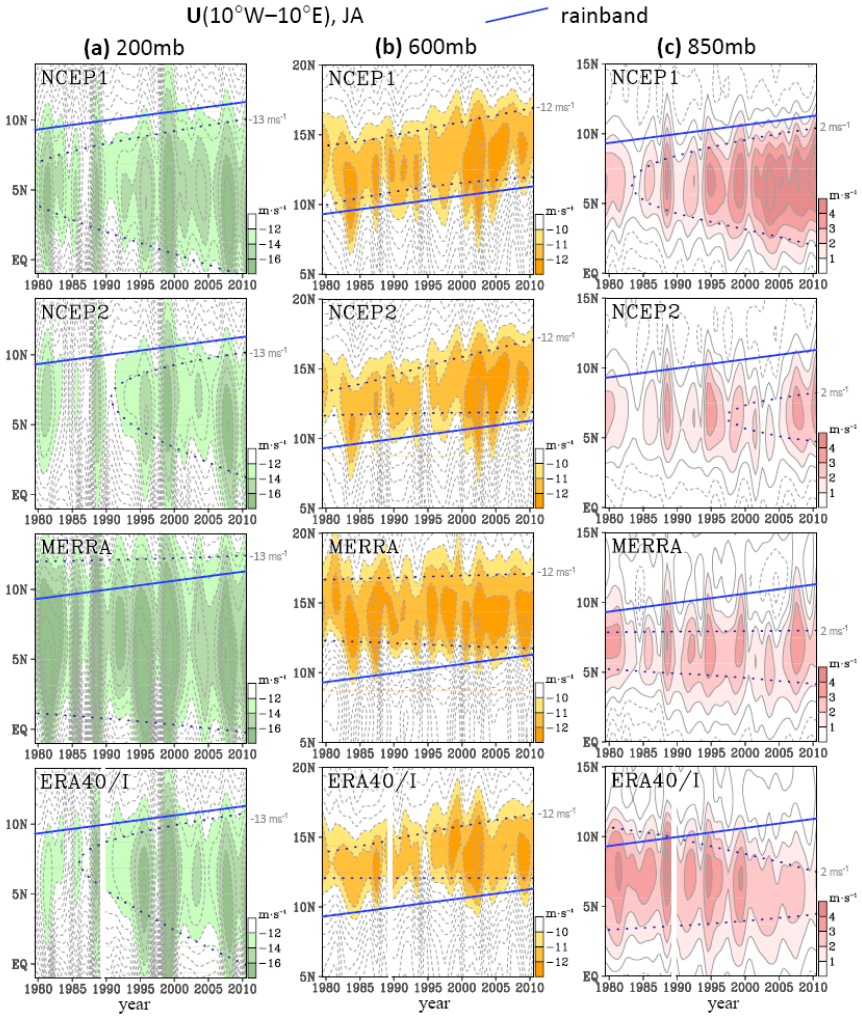

Fig. 3 Same as Fig. 2 but for zonal wind speeds at levels of (a) 200 mb, (b) 600 mb, and (c) 850 mb derived from (top-down) NCEP1, NCEP2, MERRA, and ERA40/I. The solid blue lines indicate the Sahel rainband migration. The dotted lines indicate linear trends of the designated value. Note the different latitudinal scales for each level. In ERA40/I, year 1989 is masked out to highlight the transition from ERA40 to ERA-Interim.

circulations, while newer reanalyses do not appear to correspond with each other, such as the AEJ's trend between MERRA and ERA40/I. Therefore, in the ensuing analysis we adopted an ensemble approach by averaging the four reanalyses with an equal weight, denoted as the *ensemble reanalyses*.

Recall from Fig. 2 that, although the precipitation amounts have not increased significantly, ΔOLR has intensified. The root-mean-square (RMS) of daily OLR over the central Sahel (Fig. 4a) supports this observation as it reveals an enhanced fluctuation along the northern edge of the migrating rainband (~15°N). This likely is due to the rainband moving towards the Saharan boundary where stronger potential temperature gradients and lower static stabilities are present; this subsequently leads to greater thermal and convective instabilities (discussed later). To examine the change in moist convection, we computed the frequency from which the daily OLR values at each grid point were lower than 200 Wm^{-2}, which is an empirical threshold obtained for deep convection that usually occurs over tropical oceans (Zhang 1993). The result (Fig. 4b) portrays a northward migration in the frequency of intense convection that is coupled to the migrating rainband (*i.e.* the blue line). The eastern Sahel (not shown) undergoes consistent changes in convective activity.

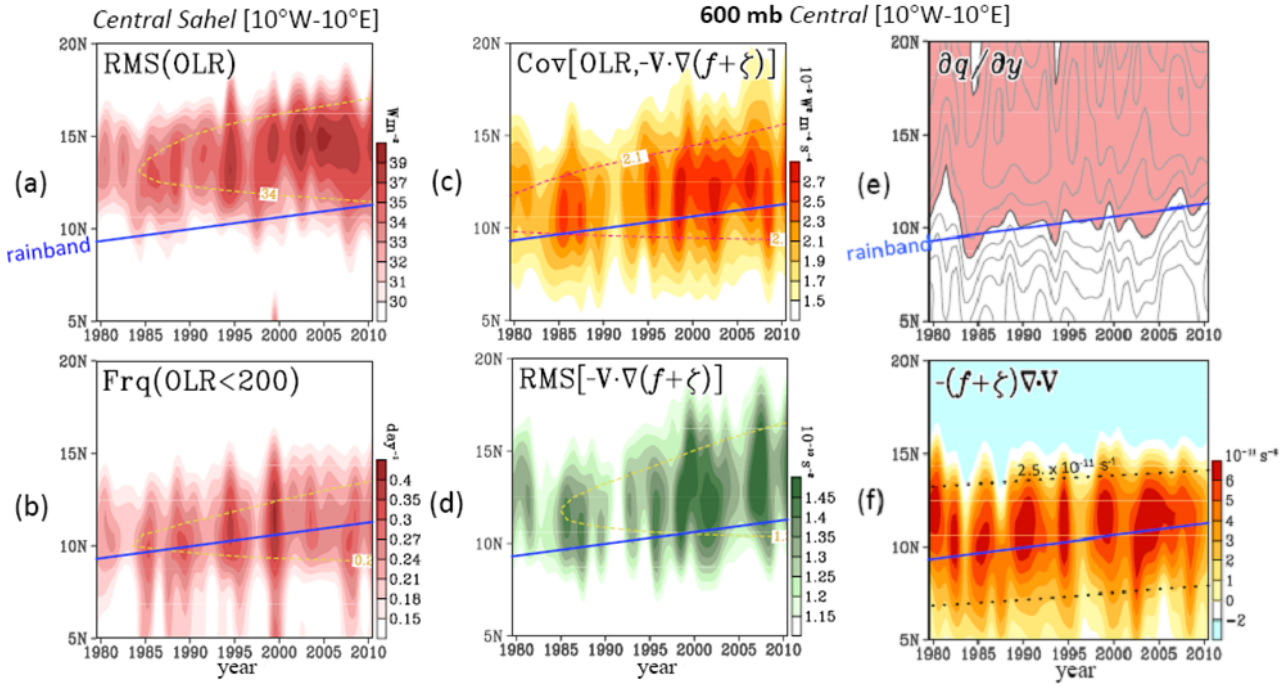

Fig. 4 Same as Fig. 3 but for (a) root-mean-square (RMS) of the 2-8 day bandpass filtered OLR, (b) frequency of the OLR values lower than 200 Wm-2, (c) covariance of the filtered OLR with horizontal vorticity advection at 600 mb, (d) RMS of the filtered horizontal vorticity advection at 600 mb, (e) meridional gradient of Ertel potential vorticity at 600 mb, and (f) vorticity source due to vortex stretching at 600 mb. Dashed lines are linear trends of the designated value. The Sahel rainband is indicated by solid blue lines.

It is known that, within the latitude zone of 10°-15°N, AEWs contribute a significant portion to the seasonal precipitation (Grist *et al.* 2002; Chen and Wang 2007). The association of the changing convective activity with AEWs was examined by calculating the covariance of the ΔOLR in conjunction with the vorticity advection forcing of vorticity tendency at 600 mb, $-\mathbf{V}\cdot\nabla(f+\zeta)$, where **V** indicates horizontal wind vectors, f is the planetary vorticity, and ζ is the relative vorticity. Both variables were bandpass filtered with 2-8 days in order to isolate the signal of AEWs. As is shown in Fig. 4c, a substantial increase and a northward position shift are observed in the covariance of ΔOLR and vorticity advection. This suggests an expansion and northward shift of the wave-convection interaction. The RMS of the filtered vorticity advection (Fig. 4d) shows a similar shift with an amplifying tendency that may be interpreted as a northward displacement of the AEW track accompanied by an amplification of those waves. The wave activity in the eastern Sahel – *i.e.* one

of the breeding zones of AEWs – is generally weaker than in the central Sahel but shows a similar tendency: a northward shift and a latitudinal expansion. Chen and Wang (2007) have noted a 20% increase in the number of "moist" AEWs that occur south of the AEJ (the so-called southern track). These results indicate that the migrating and intensifying convection, AEJ, and AEWs are connected with the shifting Sahel rainband and, that convection coupled to the AEJ-AEW system has become stronger over the northern part of the Sahel.

b. Changes in the dynamic structure

It is well established that the formation mechanism of AEWs, particularly the southern track, relies upon the Charney-Stern instability (Charney and Stern 1962) in which the meridional gradient of potential vorticity changes sign south of the AEJ and is negative underneath the AEJ (Burpee 1972; Thorncroft and Hoskins 1994a, b). The Charney-Stern instability occurs in an environment of combined thermal gradient and vertical shear that promotes the release of available potential energy (from the mean circulation) towards any pressure perturbations. Therefore, we examined the change in this dynamics through the meridional gradient of potential vorticity, dq/dy, at 600 mb (Fig. 4e). Compared with the AEJ as depicted in Fig. 3b, the sign change of dq/dy indeed occurs south of the jet while exhibits a northward progression corresponding to the AEJ's migration. Noteworthy is that the intensified AEJ may also induce stronger shear instability south of the jet; this being favorable for the development of AEWs. As has been shown previously (Chen 2006), mid-tropospheric vortex stretching is a dominant forcing source in the vorticity budget over the AEW genesis region. An examination of the seasonal mean vortex stretching at 600 mb reveals an amplifying tendency associated with a northward migration (Fig. 4f), with a more pronounced amplification in the eastern Sahel. These features correspond well with the intensification and positional shift of AEWs revealed from Figs. 4c and 4d. Since the AEW activity is positively correlated with the Sahel rainfall (on the interannual timescale; Thorncroft and Rowell 1998), these also seem to support the position shift of the Sahel rainband.

During the last 30 years, surface temperature over the Saharan desert has warmed within the range of 0.5°-1.0°C (not shown); a warming like this strengthens the heat low and lowers the static stability. The change in warming and static stability [from the combination of low static stability and a stronger meridional temperature gradient; Chang 1993] likely reinforces the heat low's interaction with the northward migrating AEJ, leading to an enhancement in baroclinic instability. When coupled with the increased moisture supply and enhanced moist convection conditions, mixed barotropic and baroclinic instabilities likely result in a stronger reversal of the mid-tropospheric potential vorticity gradient, thus enhancing dq/dy. This appears to be the case as is evident in Fig. 4e. Such processes further explain the intensified AEW-OLR activity suggested from Fig. 4c.

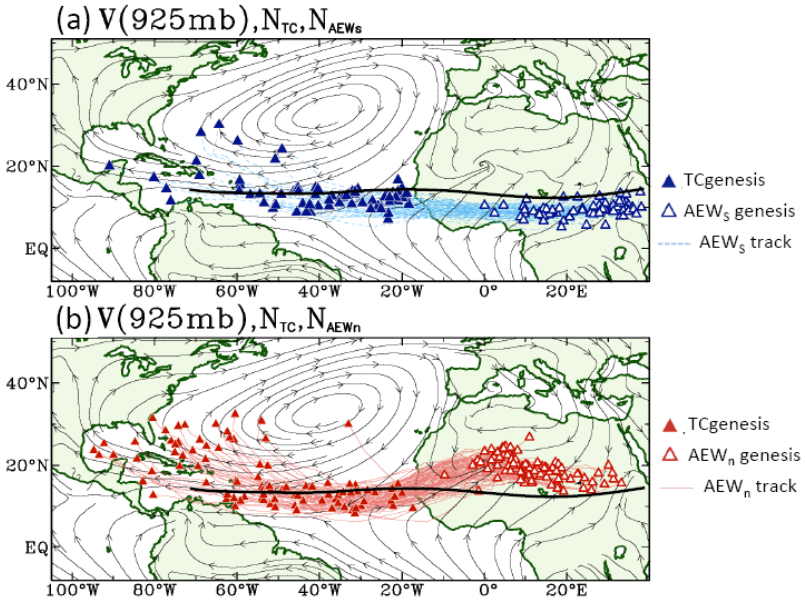

Fig. 5 July-September climatological streamlines at 925mb overlaid with tropical cyclogeneses of AEW origin and the trajectory and genesis of AEWs for (a) the southern track (AEWS) and (b) the northern track (AEWn). Symbols are explained in the right. The AEJ core is indicated by the black solid line. Data period: 1979-2006. (Modified from Chen *et al.* 2008)

c. Link with Atlantic tropical cyclones

During the past 30 years, both the frequency and the intensity of Atlantic tropical cyclones have increased significantly. A growing number of studies have suggested that tropical cyclone activity and Sahel rainfall anomalies are linked to the uptrend phase of the AMO [as reviewed by Latif *et al.* 2010], but such a linkage has not yet been substantiated. Landsea

(1993) has estimated that about 60% of tropical storms and moderate tropical cyclones in the Atlantic basin, and over 80% of intense tropical cyclones (*i.e.* Category 3 and above) originate from AEWs. Later studies (Thorncroft and Hodges 2001; Hopsch *et al.* 2007; Chen *et al.* 2008) found that southern-track AEWs contribute the most to tropical cyclogenesis, because their nature of moist convection facilitates the conversion of cold-core waves into warm-core tropical cyclones (Pytharoulis and Thorncroft 1999).

The Atlantic tropical cyclogeneses and those that originate from AEWs was examined by performing a back-tracking method of AEWs as was used in Chen *et al.* (2008). The back-tracking procedure begins with the genesis location of a tropical cyclone, then tracks any pre-existing perturbation associated with the tropical cyclogenesis *back* to its origin of perturbation by using daily-mean wind and vorticity fields at 925 mb and 600 mb in conjunction with daily OLR. Here, if the perturbation originated over the African continent, then its related tropical cyclogenesis is regarded as being of AEW origin. The tracking was performed manually and only those tropical cyclones during the period 2005-2010 were tracked, while cases prior to 2005 were adopted from Chen et al. (2008). Illustrated in Fig. 5 are tropical cyclogeneses with an AEW origin, the initial locations of those AEWs, and the trajectory between the two. Southern-track AEWs tend to form tropical cyclones further to the east and closer to West Africa than northern-track AEWs, likely due to stronger latent heat release in the West African monsoon region (Thorncroft and Hodges 2001).

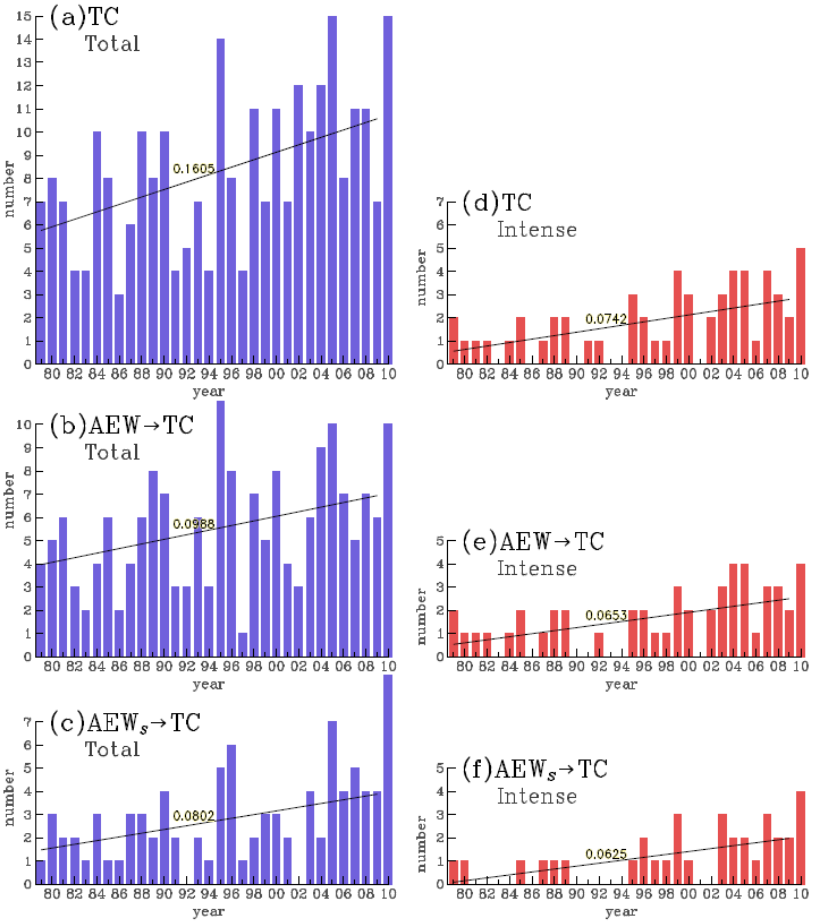

Fig. 6 Number of Atlantic tropical cyclones (TCs) during July-September, for (a) total TCs, (b) AEW-induced TCs, and (c) southern-track AEW-induced TCs. (d)-(f) Same as (a)-(c) but for intense TCs of Category 3 and above. The linear trends and slopes are given. All trends are significant at the 95% confidence interval per *t*-test.

Figure 6a shows the number of tropical cyclones initiated in the July-September season and their linear trend. Year 2010 was not included in the trend analysis because the track records at the time were provisional. Of the 86% *increase* in the number of tropical cyclones since 1979, 62% originated from AEWs (Fig. 6b) while 50% are linked to southern track AEWs (Fig. 6c). The connection between AEWs and intense tropical cyclones is more pronounced: Given a dramatic 148% *increase* in the number of intense tropical cyclones, 88% are of AEW origin (Fig. 6e), while 84% (out of the 88%) originated from the southern track of AEWs (Fig. 6f). It has been found that the large-scale atmospheric conditions leading to the increase in tropical cyclone frequency and power involve net surface radiation, thermodynamic efficiency, surface wind speed, and vertical wind shear (Emanuel 2007), whose variations turn to the favorable side for tropical cyclogenesis during the recent AMO uptrend (Hoerling *et al.* 2006; Latif *et al.* 2010). The results presented in Fig. 6 are a further substantiation of the synoptic condition that exists to "fuel" the observation of increasing rainfall in the Sahel and the Atlantic tropical cyclones (especially the intense ones).

5. Concluding remarks

Increased Sahel rainfall over the 1979-2010 period and associated synoptic conditions was found to result from the northward migration of the seasonal rainband. Convective activity associated with the migrating rainband also intensified, mostly along the northern boundary of the rainband and south of the AEJ. We also found a positional shift and intensification of the AEJ, consistent with the northward migration of the Sahel rainband. These features are accompanied by stationary tropical monsoon westerlies, an expanding TEJ, and an increase in moisture flux convergence (not shown). Furthermore, the poleward shift and amplification of AEW activity associated with the AEJ changes play a crucial role in the change of tropical cyclogenesis over the North Atlantic. Through a manual back-tracking method that connects tropical cyclones to their AEW origin, 88% of the dramatic (148%) increase in intense tropical cyclones were found to originate from AEWs. These results provide a synoptic linkage between the documented increase in tropical cyclone threat and the increasing Sahel rainfall, over the past 30 years. In view of the severe spreads in GCM projections of the Sahel climate, simulation quality in terms of the AEJ-AEW system may serve as an additional criterion for the assessment of projection uncertainties. Moreover, projected AEW activities may also provide an indication for future tropical cyclone threat.

References

Adler, R. F., and Coauthors, 2003: The Version-2 Global Precipitation Climatology Project (GPCP) Monthly Precipitation Analysis (1979,ÄìPresent). *Journal of Hydrometeorology*, **4,** 1147-1167.

Brohan, P., J. J. Kennedy, I. Harris, S. F. B. Tett, and P. D. Jones, 2006: Uncertainty estimates in regional and global observed temperature changes: A new data set from 1850. *J. Geophys. Res.*, **111,** D12106.

Burpee, R. W., 1972: The Origin and Structure of Easterly Waves in the Lower Troposphere of North Africa. *J. Atmos. Sci.*, **29,** 77-90.

Chang, C.-B., 1993: Impact of Desert Environment on the Genesis of African Wave Disturbances. *J. Atmos. Sci.*, **50,** 2137-2145.

Charney, J. G., and M. E. Stern, 1962: On the Stability of Internal Baroclinic Jets in a Rotating Atmosphere. *J. Atmos. Sci.*, **19,** 159-172.

Chen, T.-C., 2006: Characteristics of African Easterly Waves Depicted by ECMWF Reanalyses for 1991,Äì2000. *Mon. Wea. Rev.*, **134,** 3539-3566.

Chen, T.-C., S.-Y. Wang, and A. J. Clark, 2008: North Atlantic Hurricanes Contributed by African Easterly Waves North and South of the African Easterly Jet. *J. Climate*, **21,** 6767-6776.

Chen, T. C., and S.-Y. Wang, 2007: Interannual variation of the Sahel rainfall. Geophysical Research Abstracts, Vol. 9, 11206. *European Geosciences Union Symposium of Precipitation Science*.

Cook, K. H., 2008: Climate science: The mysteries of Sahel droughts. *Nature Geosci*, **1,** 647-648.

Dai, A., P. J. Lamb, K. E. Trenberth, M. Hulme, P. D. Jones, and P. Xie, 2004: The recent Sahel drought is real. *Inter. J. Climatol.*, **24,** 1323-1331.

Emanuel, K., 2005: Increasing destructiveness of tropical cyclones over the past 30 years. *Nature*, **436,** 686-688.

——, 2007: Environmental Factors Affecting Tropical Cyclone Power Dissipation. *J. Climate*, **20,** 5497-5509.

Fink, A. H., J. M. Schrage, and S. Kotthaus, 2010: On the Potential Causes of the Nonstationary Correlations between West African Precipitation and Atlantic Hurricane Activity. *J. Climate*, **23,** 5437-5456.

Giannini, A., R. Saravanan, and P. Chang, 2003: Oceanic Forcing of Sahel Rainfall on Interannual to Interdecadal Time Scales. *Science*, **302,** 1027-1030.

Grist, J. P., S. E. Nicholson, and A. I. Barcilon, 2002: Easterly Waves over Africa. Part II: Observed and Modeled Contrasts between Wet and Dry Years. *Mon. Wea. Rev.*, **130,** 212-225.

Hagos, S. M., and K. H. Cook, 2008: Ocean Warming and Late-Twentieth-Century Sahel Drought and Recovery. *J. Climate*, **21,** 3797-3814.

Herrmann, S. M., A. Anyamba, and C. J. Tucker, 2005: Recent trends in vegetation dynamics in the African Sahel and their relationship to climate. *Global Environmental Change Part A*, **15,** 394-404.

Hoerling, M., J. Hurrell, J. Eischeid, and A. Phillips, 2006: Detection and Attribution of Twentieth-Century Northern and Southern African Rainfall Change. *J. Climate*, **19,** 3989-4008.

Hopsch, S. B., C. D. Thorncroft, K. Hodges, and A. Aiyyer, 2007: West African Storm Tracks and Their Relationship to Atlantic Tropical Cyclones. *J. Climate*, **20,** 2468-2483.

Kalnay, E., and Coauthors, 1996: The NCEP/NCAR 40-Year Reanalysis Project. *Bull. Amer. Meteor. Soc.*, **77,** 437-471.

Kanamitsu, M., W. Ebisuzaki, J. Woollen, S.-K. Yang, J. J. Hnilo, M. Fiorino, and G. L. Potter, 2002: NCEP–DOE AMIP-II Reanalysis (R-2). *Bull. Amer. Meteor. Soc.*, **83,** 1631-1643.

Knight, J. R., R. J. Allan, C. K. Folland, M. Vellinga, and M. E. Mann, 2005: A signature of persistent natural thermohaline circulation cycles in observed climate. *Geophys. Res. Lett.*, **32,** L20708.

Landsea, C. W., 1993: A Climatology of Intense (or Major) Atlantic Hurricanes. *Mon. Wea. Rev.*, **121,** 1703-1713.

Landsea, C. W., and W. M. Gray, 1992: The Strong Association between Western Sahelian Monsoon Rainfall and Intense Atlantic Hurricanes. *J. Climate*, **5,** 435-453.

Landsea, C. W., N. C. C. Anderson, G. Clark, J. Dunion, J. Fernandez-Partagas, P. Hungerford, C., and a. M. Z. Neumann, 2004: The Atlantic hurricane database re-analysis project: Documentation for the 1851-1910 alterations and additions to the HURDAT database. *Hurricanes and Typhoons: Past, Present and Future*, R. J. M. a. K.-B. Liu, Ed., Columbia University Press, 177-221.

Latif, M., and Coauthors, 2010: Dynamics of decadal climate variability and implications for its prediction. *OceanObs'09: Sustained Ocean Observations and Information for Society*, Venice, Italy.

Legates, D. R., and C. J. Willmott, 1990: Mean seasonal and spatial variability in gauge-corrected, global precipitation. *Int. J. Climatol.*, **10,** 111-127.

Lu, J., and T. L. Delworth, 2005: Oceanic forcing of the late 20th century Sahel drought. *Geophys. Res. Lett.*, **32,** L22706.

Nicholson, S., and X. Yin, 2001: Rainfall Conditions in Equatorial East Africa during the Nineteenth Century as Inferred from the Record of Lake Victoria. *Climatic Change*, **48,** 387-398.

Olsson, L., L. Eklundh, and J. Ardˆ, 2005: A recent greening of the Sahel--trends, patterns and potential causes. *Journal of Arid Environments*, **63,** 556-566.

Pytharoulis, I., and C. Thorncroft, 1999: The Low-Level Structure of African Easterly Waves in 1995. *Mon. Wea. Rev.*, **127,** 2266-2280.

Rienecker, M. M., and Coauthors, 2011: MERRA - NASA's Modern-Era Retrospective Analysis for Research and Applications. *J. Climate,* in press.

Schimel, D. S., and Coauthors, 2001: Recent patterns and mechanisms of carbon exchange by terrestrial ecosystems. *Nature*, **414,** 169-172.

Simmons, A. S., D. D. Uppala, and S. Kobayashi, 2007: ERA-interim: new ECMWF reanalysis products from 1989 onwards. *CMWF Newsl* **110,** 29-35.

Smith, T. M., and R. W. Reynolds, 2003: Extended Reconstruction of Global Sea Surface Temperatures Based on COADS Data (1854,Äì1997). *J. Climate*, **16,** 1495-1510.

Thorncroft, C., and K. Hodges, 2001: African Easterly Wave Variability and Its Relationship to Atlantic Tropical Cyclone Activity. *J. Climate*, **14,** 1166-1179.

Thorncroft, C. D., and B. J. Hoskins, 1994a: An idealized study of African easterly waves. I: A linear view. *Quarterly Journal of the Royal Meteorological Society*, **120,** 953-982.

——, 1994b: An idealized study of African easterly waves. II: A nonlinear view. *Quarterly Journal of the Royal Meteorological Society*, **120,** 983-1015.

Thorncroft, C. D., and D. P. Rowell, 1998: Interannual variability of African wave activity in a general circulation model. *Inter. J. Climatol.*, **18,** 1305-1323.

Uppala, S. M., and Coauthors, 2005: The ERA-40 re-analysis. *Quarterly Journal of the Royal Meteorological Society*, **131,** 2961-3012.

Wang, S.-Y., and R. R. Gillies, 2011: Observed change in Sahel rainfall, circulations, African easterly waves, and Atlantic hurricanes since 1979. *International Journal of Geophysics***,** (in press) doi:10.1155/2011/259529.

Xie, P., and P. A. Arkin, 1997: Global Precipitation: A 17-Year Monthly Analysis Based on Gauge Observations, Satellite Estimates, and Numerical Model Outputs. *Bull. Amer. Meteor. Soc.*, **78,** 2539-2558.

Zhang, C., 1993: Large-Scale Variability of Atmospheric Deep Convection in Relation to Sea Surface Temperature in the Tropics. *J. Climate*, **6,** 1898-1913.